Thesis for the Degree of Master of Engineering

Control for Mobile Inverted Pendulum Using Sliding Mode Technique

by

Ming Tao Kang

Department of Interdisciplinary of Mechatronics Engineering

Graduate School

Pukyong National University

August 2007

Control for Mobile Inverted Pendulum Using Sliding Mode Technique

슬라이딩모드법을 이용한 주행형도립진자의 제어

Advisor: Prof. Sang Bong Kim

by

Ming Tao Kang

A Thesis Submitted in Partial Fulfillment of the Requirements for the Degree of

Master of Engineering

**In Department of Interdisciplinary of Mechatronics Engineering,
Graduate School,
Pukyong National University**

August 2007

Control for Mobile Inverted Pendulum Using Sliding Mode Technique

A dissertation
by

Ming Tao Kang

Approved by:

Chairman Prof. Young Joo An

Member Prof. Inpil Kang

Member Prof. Sang Bong Kim

August 27, 2007

Acknowledgments

I would like to take this opportunity to express my sincere appreciation and deepest gratitude to all those who helped me throughout my graduate studies. This thesis could not have been completed without their help and continuous support.

First and foremost, I would like to express my sincere gratitude to my supervisor, Prof. Sang Bong Kim, Pukyong National University. He has been a source of inspiration and ideas, given me great challenges and been very supportive with all kinds of help.

I would like to appreciate the members of this thesis committee, Prof. Inpil Kang and Prof. Young Joo An, for their detailed comments and suggestion during the phases of the preparation of this thesis.

I would like to thank Prof. Hak Kyeong Kim, Dr. Tan Lam Chung, Dr. Manh Dung Ngo, Dr. Hoang Duy Vo and PhD. candidate Nguyen Thanh Phuong, who gave me a great deal of help to complete this thesis.

I am grateful to all members of CIMEC Lab. for giving me a comfortable and active environment to achieve my study: Ms. Hee Suk Lee, Mr. Sang Chan Kim, Mr. Seong Jin Ma, Mr. Ba Da Park, Mr. Byoung Yong Kim, Mr. Joon Ho Jeong, Mr. Suk Min Yoon, Mr. Do Kyoung Lee, Mr. Nak Soon Choi, Mr. Dae Won Kim and Mr. Jeong Woo Park, who have helped me a lot when I put the first step here to be aware of Korea life and the activities in Lab. Moreover, I would like to thank Chinese students in Pukyong National University, Gang Niu, Xiao Di, Ting Wen and all my friends for their encouragement.

Last but not least, it is my pleasure to thank my parents, my sister, my brother-in-law and my brother. Their patience, support and impeccable understanding allowed me to write this thesis.

Ming Tao Kang

TO OUR PARENTS

獻給親愛的父母

Contents

Control for Mobile Inverted Pendulum Using Sliding Mode Technique

Ming Tao Kang

Department of Interdisciplinary of Mechatronics Engineering
Graduate School
Pukyong National University

Abstract

In this thesis, a mobile inverted pendulum system is considered. A control system pilots the motors so as to keep the system in equilibrium. The mobile inverted pendulum is a system with an inverted pendulum attached to a mobile cart with two coaxial wheels, each of which is coupled to a DC motor. The dynamic equation of the mobile inverted pendulum is established. To stabilize the mobile inverted pendulum, a stabilizing controller via sliding mode control is designed based on Ackermann's formula, which obtains a sliding surface in explicit form as well. The control law is designed to make quick converge to the state of the closed-loop system during the control process. The overall control system is described. The servo controller using two microcontrollers PIC16F877 is introduced. Moreover, the configuration using Lyapunov function is presented to control the speed of a DC motor. A configuration for sensors including tilt sensor and two incremental encoders is developed to obtain the system states and

realize the above proposed controller. These measurements can then be fed back to the controllers to impose the desired closed loop dynamics. The simulation and experimental results are shown to prove the effectiveness of the proposed modeling and the stabilizing controller.

Nomenclature

Variable	Description	Units
x_r	Position of the cart	$[m]$
x_d	Desired position of the cart	$[m]$
V_e	Back electromotive force voltage	$[V]$
K_e	Back electromotive force voltage constant	$[V \cdot \sec / rad]$
K_m	Torque constant of motor	$[Nm / A]$
R	Nominal terminal resistance	$[\Omega]$
θ	Rotational angle of motor shaft	$[rad]$
ω	Angular velocity of motor shaft	$[rad / \sec]$
θ_{Lw}, θ_{Rw}	Rotational angle of left or right wheel	$[rad]$
H_{fL}, H_{fR}	Friction force between the ground and left/right wheel	$[N]$
$H_L, P_L; H_R, P_R$	Reaction forces between left/right wheel and pendulum	$[N]$
T_L, T_R	Load torque to left and right wheel	$[N \cdot m]$
T_a	Applied load torque	$[N \cdot m]$
T_m	Electric motor torque	$[N \cdot m]$
V	Applied voltage for left and right wheel motor	$[V]$
I_R	Rotor inertia of motor	$[kg \cdot m^2]$
L_i	Rotor inductance of motor	$[H]$
K_f	Frictional constant	$[N \cdot m \cdot \sec / rad]$
i	Armature current	$[A]$
θ_w	Angular velocity of wheel	$[rad / \sec]$

I_w	Moment of inertia of the wheel	$[Kg \cdot m^2]$
I_p	Moment of inertia of pendulum around z axis	$[Kg \cdot m^2]$
M_w	Mass of the wheel	$[Kg]$
M_p	Mass of the inverted pendulum	$[Kg]$
r	Wheel radius	$[m]$
φ	Rotation angle around z axis of the pendulum	$[rad]$
δ	Rotation angle around y axis of the pendulum	$[rad]$
D	Lateral distance between the wheels	$[m]$
L	Distance between the wheel's center and the pendulum's center of gravity	$[m]$
g	Gravitational acceleration	$[m/\sec^2]$

1

Introduction

1.1 Background and Motivation

Inverted pendulum systems always exhibit many problems in industrial applications, for example, various nonlinear behaviors under different operation conditions, external disturbances, and physical constraints on some variables. Therefore, the task of real time stabilization and tracking control of a highly nonlinear unstable mobile inverted pendulum system has been a challenge for the modern control field.

A mobile inverted pendulum is a system composed of an inverted pendulum attached to a mobile cart with two coaxial wheels, each of which is coupled to a DC motor.

There are some studies that have been reported on the mobile inverted pendulum as follow:

Prof. Kazuo Yamafuzi, at University of Electro-Communications, built the first two-wheel inverted pendulum robot in 1986.

A similar and commercially available system, ‘SEGWAY HT’ has been invented by Dean Kamen as shown in Fig. 1.1. The ‘SEGWAY HT’ is able to balance a human standing on its platform while the user traverses the terrain with it. This innovation uses five gyroscopes and a collection of other tilt sensors to keep itself upright. Only three gyroscopes are needed for the whole system, and the additional sensors are included as a safety precaution.

In 2002, Felix Grasser et al. [1] at the Industrial Electronics Laboratory of the Swiss Federal Institute of Technology have built a scaled down prototype JOE as

shown in Fig. 1.2. The vehicle is composed of a cart carrying a DC motor coupled to a planetary gearbox for each wheel, the digital signal processor (DSP) board used to implement the controller, the power amplifiers for the motors, and the necessary sensors to measure the system states.

Fig. 1.1 SEGWAY HT

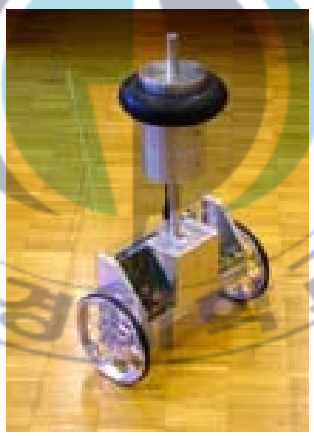

Fig. 1.2 JOE

The uniqueness of the system has drawn interest from robot enthusiasts. For example, Nbot, a two-wheeled robot built by David P. Anderson, uses an inertial sensor and motor encoder to balance the system as shown in Fig. 1.3.

Fig. 1.3 Nobt

To guarantee the inverted pendulum in equilibrium, the development of the control system is vital. Recently, the control problems of inverted pendulum have been intensively studied due to the challenging demand of fast and precise performance. The control strategies for the inverted pendulum in the literature can be divided into two distinct sections, namely linear control and nonlinear control.

The linear control methods often linearize the dynamics about a certain operation point. The linear controllers are more popular among researchers designing the mobile inverted pendulum like JOE. The pole-placement controller and the linear quadratic regulators (LQR) are the popular method implemented.

In 1994, Tarek et al. developed a Fuzzy Logic controller for stabilizing an inverted pendulum on a cart. This approach is based on approximate reasoning and knowledge based control. In 1991, Williams and Matsuoka [2] used the inverted pendulum to demonstrate the ability of Neural Networks controller in controlling nonlinear unstable systems.

Although nonlinear controllers would provide a more robust system, the complexity and difficulties of these methods make most researchers utilize the linear controller approach [3-17].

Sliding mode control method is a robust control method which generates an input to track a desired trajectory for a given system. In the past decade, the sliding mode control has been widely used in various practical applications.

In 1998, Juergen Ackmann and Vadim Utkim [18] designed a sliding mode controller based on Ackermann's Formula. While simulation results prove that the mobile inverted pendulum can be balanced by this controller, there is no evidence of implementing this controller.

In this thesis, the control objective is to implement a sliding mode controller to stabilize the mobile inverted pendulum.

1.2 Outline and Summary of Contributions

This thesis consists of six chapters. The content and summary of contributions in each chapter are summarized as follows:

- **Chapter 1: Introduction**

  Background and motivation, the outline and summary of contributions of this research are presented.

- **Chapter 2: Mathematical Modeling**

  Mathematical models of the mobile inverted pendulum and the DC motor are presented when the movement of the mobile inverted pendulum is restricted in a plane.

- **Chapter 3: Controller Design**

  A stabilizing controller via sliding mode control using Ackermann's formula is presented to stabilize the mobile inverted pendulum. The control law is designed to make quick converge to the state of the closed-loop system during the control process.

- **Chapter 4: Hardware Design and Implementation**

The overall control system is described. A servo controller using two microcontrollers PIC16F877 is introduced. Moreover, the configuration using Lyapunov function to control the speed of DC motor is presented.

- **Chapter 5: Simulation and Experimental Results**

  The simulation and experimental results are shown to prove the effectiveness of the proposed modeling and the stabilizing controller.

- **Chapter 6: Conclusions and Future Work**

  Summary this thesis results and the future work.

2

Mathematical Modeling

The mathematical models for the mobile inverted pendulum and the motor are derived in this chapter.

2.1 Modeling of DC Motor

The mobile inverted pendulum is powered by two DC motors. In this section, the motor dynamics is derived. This model is then used in the dynamic modeling of the mobile inverted pendulum to provide a relationship between the input voltage of the motors and the torque needed to the system.

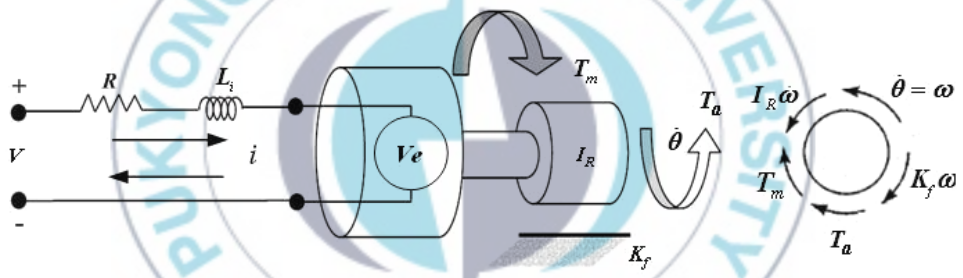

Fig. 2.1 Diagram of DC Motor

Fig. 2.1 shows the cut from a mechanical load as well as the cut from a DC power supply. The conversion of the electrical energy from the DC power supply into the mechanical energy supplied to the load takes place in the DC motor.

When a voltage V is applied to the terminals of the motor, a current i will flow in the motor armature. The motor produces a torque T_m, which is proportional to the current. This relationship can be expressed as

$$T_m = K_m i \tag{2.1}$$

A resistor-inductor pair in series with a voltage V_e can be used to model the electrical circuit of the motor. This back electromotive force voltage is produced because the coils of the motor are moving through a magnetic field. The back EMF can be approximated as a linear function of shaft velocity, which can be written as

$$V_e = K_e \omega \tag{2.2}$$

At this point, a linear differential equation for the DC motor's electrical circuit can be written by using Kirchoff's Voltage Law that the sum of all voltages in the circuit must be equal to zero. For the DC motor, this can be written as

$$V - Ri - L_i \frac{di}{dt} - V_e = 0 \tag{2.3}$$

In deriving the equation of motion for the motor, the friction on the shaft of the motor is approximated as a linear function of the shaft velocity. The approximation that the friction coefficient on the shaft of the motor K_f is a linear function of the shaft velocity is made. In Fig. 2.1, Newton's law of motion states that the sum of all torques produced on the shaft is linearly proportional to the acceleration of the shaft by the inertial moment of armature I_R. The preceding statement can be written as

$$I_R \frac{d\omega}{dt} = T_m - K_f \omega - T_a \tag{2.4}$$

Substituting equations (2.1) and (2.2) into equations (2.3) and (2.4), and rearranging in terms of the time derivatives, two fundamental equations governing the motion of the motor can be obtained as

$$\frac{di}{dt} = \frac{V}{L_i} - \frac{R}{L_i} i - \frac{K_e}{L_i} \omega \tag{2.5}$$

$$\frac{d\omega}{dt} = \frac{K_m}{I_R} i - \frac{K_f}{I_R} \omega - \frac{T_a}{I_R} \tag{2.6}$$

Both equations are linear function of current and shaft velocity, and they include the first order time derivatives. To simplify DC motor model applied to the mobile inverted pendulum, the motor inductance and the motor friction are negligible and current derivative can be given as zero. Hence, equations (2.5) and (2.6) can be approximated as

$$i = \frac{V}{R} - \frac{K_e}{R} \omega \tag{2.7}$$

$$\frac{d\omega}{dt} = \frac{K_m}{I_R} i - \frac{T_a}{I_R} \tag{2.8}$$

By substituting equation (2.7) into equation (2.8), an approximation for the DC motor which is only a function of the shaft velocity, applied voltage and load torque can be obtained as

$$\frac{d\omega}{dt} = -\frac{K_m K_e}{I_R R} \omega + \frac{K_m}{I_R R} V - \frac{T_a}{I_R} \tag{2.9}$$

Since the motor inductance is neglected, the current through the windings is not considered in the equation of motion of the motor. The current will reach a constant state immediately compared to the velocity of the shaft, which takes time to speed up from some initial velocity to a final velocity after a change in the input voltage.

From equation (2.9), the equation can be obtained as follows:

$$I_R \frac{d\omega}{dt} + T_a = -\frac{K_m K_e}{R}\omega + \frac{K_m}{R}V \tag{2.10}$$

This is a system of the first order differential equations with respect to shaft velocity of the motor ω. The input to the motor is the applied voltage.

From equation (2.4) under the above conditions, the motor torque equation can be obtained as follows:

$$T_m = I_R \frac{d\omega}{dt} + T_a \tag{2.11}$$

2.2 Dynamic Modeling of the Mobile Inverted Pendulum

The mobile inverted pendulum has similar behavior with an inverted pendulum on a mobile cart. The mobile inverted pendulum is restricted to a plane in order to facilitate the development of a control system. The inverted pendulum and wheel dynamics are analyzed separately at the beginning, but this eventually leads to two equations of motion which describes the behavior of the mobile inverted pendulum. It is assumed that the wheels always stay in contact with the ground and that there is no slip at the wheel's contact point. Therefore, there is no movement in the z axis and no rotation about the x axis. The left and right wheels are completely analogous. Additionally, cornering forces are negligible.

The system was developed by Felix Grasser et al. Fig. 2.2 shows the mobile inverted pendulum. In this thesis, its movement is described by the rotational angle φ and the corresponding angular velocity $\dot{\varphi}$; the linear movement of the cart is characterized by the position x_r and the velocity $\dot{x}_r$.

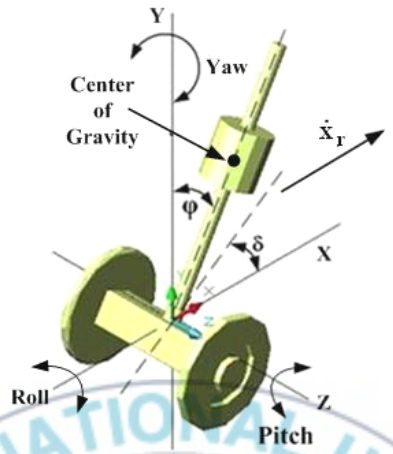

Fig. 2.2 Definition of State-space Variables

2.2.1 Wheel Dynamics

Since the system's behavior can be influenced by disturbances as well as the torque from the motor, the mathematical model has to adapt to such forces. Firstly the equations of motion are associated with the left and right wheels. Fig. 2.3 shows the free body diagram for the mobile inverted pendulum. Since the equation for left and right wheels are completely analogous, only the equation for the right wheel is given.

Using the Newton's law of motion, the relation of the forces on the horizontal direction is

$$M_w \ddot{x}_r = H_{fR} - H_R \tag{2.12}$$

The relation of moments around the center of the wheel is

$$I_w \ddot{\theta}_{Rw} = T_R - H_{fR} r \tag{2.13}$$

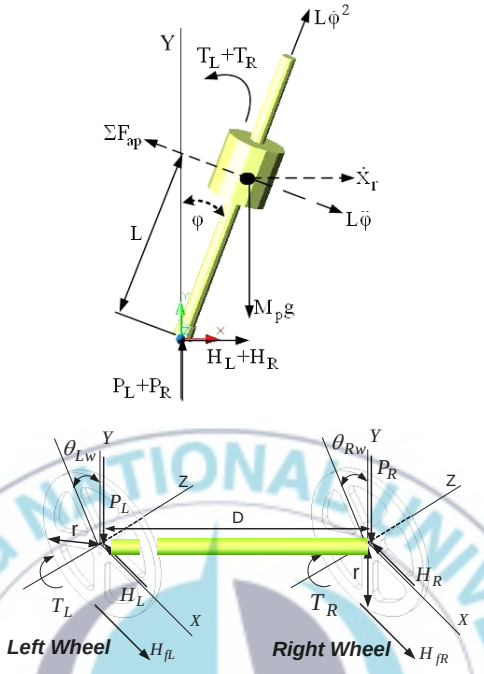

Fig. 2.3 Free Body Diagram of the Mobile Inverted Pendulum

From equations (2.10) and (2.11), the output torque to the wheels is obtained as

$$T_R = T_m = \frac{-K_m K_e}{R}\dot{\theta}_{Rw} + \frac{K_m}{R}V \tag{2.14}$$

$$|T_m| > \frac{|M_p L g \sin\varphi|}{2}$$

Therefore, equation (2.13) becomes

$$I_w \ddot{\theta}_{Rw} = \frac{-K_m K_e}{R} \dot{\theta}_{Rw} + \frac{K_m}{R} V - H_{fR} r \tag{2.15}$$

Arranging equation (2.15) yields

$$H_{fR} = \frac{-K_m K_e}{Rr} \dot{\theta}_{Rw} + \frac{K_m}{Rr} V - \frac{I_w}{r} \ddot{\theta}_{Rw} \tag{2.16}$$

Equation (2.16) is substituted into equation (2.12) to get the equation for the left and right wheels as follows:

The left wheel dynamics is

$$M_w \ddot{x}_r = \frac{-K_m K_e}{Rr} \dot{\theta}_{Lw} + \frac{K_m}{Rr} V - \frac{I_w}{r} \ddot{\theta}_{Lw} - H_L \tag{2.17}$$

The right wheel dynamics is

$$M_w \ddot{x}_r = \frac{-K_m K_e}{Rr} \dot{\theta}_{Rw} + \frac{K_m}{Rr} V - \frac{I_w}{r} \ddot{\theta}_{Rw} - H_R \tag{2.18}$$

Because the linear motion is acting on the center of the wheel, the angular rotation can be transformed into linear motion by simple transformation,

$$\ddot{\theta}_w r = \ddot{x}_r \Rightarrow \ddot{\theta}_w = \frac{\ddot{x}_r}{r}$$

$$\dot{\theta}_w r = \dot{x}_r \Rightarrow \dot{\theta}_w = \frac{\dot{x}_r}{r}$$

By the linear transformation, the left wheel dynamics (2.17) is obtained as

$$M_w \ddot{x}_r = \frac{-K_m K_e}{Rr^2} \dot{x}_r + \frac{K_m}{Rr} V - \frac{I_w}{r^2} \ddot{x}_r - H_L \tag{2.19}$$

The right wheel dynamics equation (2.18) is obtained as

$$M_w \ddot{x}_r = \frac{-K_m K_e}{Rr^2} \dot{x}_r + \frac{K_m}{Rr} V - \frac{I_w}{r^2} \ddot{x}_r - H_R \tag{2.20}$$

Adding equations (2.19) and (2.20) together yields

$$2(M_w + \frac{I_w}{r^2})\ddot{x}_r = \frac{-2K_m K_e}{Rr^2} \dot{x}_r + \frac{2K_m}{Rr} V - (H_L + H_R) \tag{2.21}$$

2.2.2 Inverted Pendulum Dynamics

The system's body can be modeled as an inverted pendulum as shown in Fig. 2.3.

The relation of the forces in the horizontal direction of the inverted pendulum is expressed as

$$(H_L + H_r) - M_p L\ddot{\varphi}\cos\varphi + M_p L\dot{\varphi}^2 \sin\varphi = M_p \ddot{x}_r \tag{2.22}$$

Arranging equation (2.22) yields

$$(H_L + H_r) = M_p \ddot{x}_r + M_p L\ddot{\varphi}\cos\varphi - M_p L\dot{\varphi}^2 \sin\varphi \tag{2.23}$$

The relation of the forces perpendicular to the pendulum can be given as

$$(H_L + H_R)\cos\varphi + (P_L + P_R)\sin\varphi - M_p g \sin\varphi - M_p L\ddot{\varphi} = M_p \ddot{x}_r \cos\varphi \tag{2.24}$$

The relation of the moments around the center of mass of pendulum can be represented as

$$-(H_L + H_R)L\cos\varphi - (P_L + P_R)L\sin\varphi - (T_L + T_R) = I_p\ddot{\varphi} \tag{2.25}$$

The torque applied on the pendulum from the motor using equation (2.14) linear transformation can be expressed into

$$T_L + T_R = \frac{-2K_mK_e}{R}\frac{\dot{x}_r}{r} + \frac{2K_m}{R}V$$

Substituting this into equation (2.25) yields

$$-(H_L + H_R)L\cos\varphi - (P_L + P_R)L\sin\varphi - (\frac{-2K_mK_e}{Rr}\dot{x}_r + \frac{2K_m}{R}V) = I_p\ddot{\varphi}$$

Arranging this yields

$$-(H_L + H_R)L\cos\varphi - (P_L + P_R)L\sin\varphi = \frac{-2K_mK_e}{Rr}\dot{x}_r + \frac{2K_m}{R}V + I_p\ddot{\varphi} \tag{2.26}$$

Multiplying equation (2.24) by $-L$ can be obtained as follows:

$$-(H_L + H_R)L\cos\varphi - (P_L + P_R)L\sin\varphi + M_pgL\sin\varphi + M_pL^2\ddot{\varphi} = -M_p\ddot{x}_rL\cos\varphi \tag{2.27}$$

Substituting equation (2.26) in equation (2.27) then yields

$$I_p\ddot{\varphi} - \frac{2K_mK_e}{Rr}\dot{x}_r + \frac{2K_m}{R}V + M_pgL\sin\varphi + M_pL^2\ddot{\varphi} = -M_pL\ddot{x}_r\cos\varphi \qquad (2.28)$$

To eliminate $(H_L + H_R)$ from the motor dynamics, substituting equation (2.23) into equation (2.21) yields

$$2(M_w + \frac{I_w}{r^2})\ddot{x}_r = -\frac{2K_mK_e}{Rr^2}\dot{x}_r + \frac{2K_m}{Rr}V - M_p\ddot{x}_r - M_pL\ddot{\varphi}\cos\varphi + M_pL\dot{\varphi}\sin\varphi \qquad (2.29)$$

Rearranging equations (2.28) and (2.29) gives the nonlinear equations of motion of the system as follows:

$$(I_p + M_pL^2)\ddot{\varphi} - \frac{2K_mK_e}{Rr}\dot{x}_r + \frac{2K_m}{R}V + M_pgL\sin\varphi = -M_pL\ddot{x}_r\cos\varphi \qquad (2.30)$$

$$\frac{2K_m}{Rr}V = (2M_w + \frac{2I_w}{r^2} + M_p)\ddot{x}_r + \frac{2K_mK_e}{Rr^2}\dot{x}_r + M_pL\ddot{\varphi}\cos\varphi - M_pL\dot{\varphi}^2\sin\varphi \qquad (2.31)$$

The above two equations can be linearized by assuming $\varphi = \pi + \phi$, where ϕ represents a small angle from the vertical upward direction.

To linearize (2.30) and (2.31), the following are assumed:

$$\cos\varphi = -1,\ \sin\varphi = -\phi \text{ and } \left(\frac{d\varphi}{dt}\right)^2 = 0$$

The equations (2.30) and (2.31) are expressed into

$$(I_p + M_p L^2)\ddot{\phi} - \frac{2K_m K_e}{Rr}\dot{x}_r + \frac{2K_m}{R}V - M_p gL\phi = M_p L\ddot{x}_r \tag{2.32}$$

$$\frac{2K_m}{Rr}V = \left(2M_w + \frac{2I_w}{r^2} + M_p\right)\ddot{x}_r + \frac{2K_m K_e}{Rr^2}\dot{x}_r - M_p L\ddot{\phi} \tag{2.33}$$

In order to get the state space representation of the system, equations (2.32) and (2.33) are rearranged as follows:

$$\ddot{\phi} = \frac{M_p L}{(I_p + M_p L^2)}\ddot{x}_r + \frac{2K_m K_e}{Rr(I_p + M_p L^2)}\dot{x}_r - \frac{2K_m}{R(I_p + M_p L^2)}V + \frac{M_p gL}{(I_p + M_p L^2)}\phi \tag{2.34}$$

$$\ddot{x}_r = \frac{2K_m}{Rr(2M_w + \frac{2I_w}{r^2} + M_p)}V - \frac{2K_m K_e}{Rr^2(2M_w + \frac{2I_w}{r^2} + M_p)}\dot{x}_r + \frac{M_p L}{2M_w + \frac{2I_w}{r^2} + M_p}\ddot{\phi} \tag{2.35}$$

By substituting equation (2.34) into equation (2.33) and substituting equation (2.35) into equation (2.32), the state space equation for the system is obtained as follows:

$$\begin{bmatrix} \dot{x}_r \\ \ddot{x}_r \\ \dot{\phi} \\ \ddot{\phi} \end{bmatrix} = \begin{bmatrix} 0 & 1 & 0 & 0 \\ 0 & a_{22} & a_{23} & 0 \\ 0 & 0 & 0 & 1 \\ 0 & a_{42} & a_{43} & 0 \end{bmatrix} \begin{bmatrix} x_r \\ \dot{x}_r \\ \phi \\ \dot{\phi} \end{bmatrix} + \begin{bmatrix} 0 \\ b_2 \\ 0 \\ b_4 \end{bmatrix} V \tag{2.36}$$

where $a_{22}, a_{23}, a_{42}, a_{43}, b_2$ and b_4 are defined as a function of the system's parameters, which is given as follows:

$$a_{22} = \frac{2K_m K_e (M_p Lr - I_p - M_p L^2)}{Rr^2 \alpha}$$

$$a_{23} = \frac{M_p^2 g L^2}{\alpha}$$

$$a_{42} = \frac{2K_m K_e (r\beta - M_p L)}{Rr^2 \alpha}$$

$$a_{43} = \frac{M_p g L \beta}{\alpha}$$

$$b_2 = \frac{2k_m (I_p + M_p L^2 - M_p Lr)}{\mathrm{R}\, r\alpha}$$

$$b_4 = \frac{2K_m (M_p L - r\beta)}{Rr\alpha}$$

$$\beta = (2M_w + \frac{2I_w}{r^2} + M_p)$$

$$\alpha = \left[I_p \beta + 2M_p L^2 (M_w + \frac{I_w}{r^2}) \right].$$

3

Controller Design

3.1 Sliding Mode Stabilizing Controller

In this section, the controller design method based upon Ackermann's formula is proposed [18]. This controller design method obtains a sliding surface equation in explicit form as well.

The procedure to design the following two controllers is introduced. First, a static controller is designed to force sliding modes to have the desired dynamic properties after a finite time interval. Then a dynamic controller that exhibits the desired dynamic properties during the entire control process is designed.

Equation (2.36) can be expressed by a differential equation as follows:

$$\dot{x} = Ax + bu \tag{3.1}$$

$$A = \begin{bmatrix} a_{11} & a_{12} & a_{13} & a_{14} \\ a_{21} & a_{22} & a_{23} & a_{24} \\ a_{31} & a_{32} & a_{33} & a_{34} \\ a_{41} & a_{42} & a_{43} & a_{44} \end{bmatrix}, \; b = \begin{bmatrix} b_1 \\ b_2 \\ b_3 \\ b_4 \end{bmatrix}, \; x = \begin{bmatrix} x_1 \\ x_2 \\ x_3 \\ x_4 \end{bmatrix}$$

where u is a scalar control.

The control law u consists of two components as follows:

$$u = u_a + u_1 \tag{3.2}$$

where u_a is static controller referred as the continuous control component and dynamic controller u_1 is the discontinuous sliding mode component. First, a state feedback law for u_a and dynamic controller u_1 are designed to enforce a sliding mode in the sliding surface based upon Ackermann's formula.

From equations (3.1) and (3.2), the following is obtained

$$\dot{x} = Ax + b(u_a + u_1)$$

$$\dot{x} = Ax + bu_a + bu_1 \tag{3.3}$$

i) Static Controller Design

The static system of equation (3.3) is nominal system and is obtained as

$$\dot{x} = Ax + bu_a \tag{3.4}$$

The static controller of equation (3.4) is given by Ackermann's formula as follows:

$$u_a = -k^T x, \;\; k^T = h^T P(A) \tag{3.5}$$

$$h^T = [0,0,0,1]\left[b, Ab, A^2b, A^3b\right]^{-1}$$

$$P(\lambda) = (\lambda - \lambda_1)(\lambda - \lambda_2)(\lambda - \lambda_3)(\lambda - \lambda_4)$$

where $\lambda_1, \lambda_2, \lambda_3, \lambda_4$ are assigned as the desired eigenvalues and $P(\lambda)$ is characteristic polynomial of equation (3.4).

From equations (3.4) and (3.5), the closed loop system is obtained as follows:

$$\dot{x} = \left(A - bk^T\right)x \tag{3.6}$$

To stabilize equation (3.6), the real parts of all eigenvalues of $\left(A - bk^T\right)$ can be assigned as negative value.

The design of sliding mode control implies choosing a sliding surface and then getting the control law enforcing sliding mode in this sliding surface.

The equation of sliding surface is chosen as

$$S = C^T x \tag{3.7}$$

where $C^T = \begin{bmatrix} c_1 & c_2 & c_3 & c_4 \end{bmatrix}^T$ with an explicit from using Ackermann's formula.

By controllability of (A, b), there exists a state feedback gain vector k that assigns the eigenvalues $\lambda_1, \lambda_2, \lambda_3, \lambda_4$ to $A - bk^T$ such that the left eigenvector C^T of $A - bk^T$ associated with λ_4 satisfies the following

$$C^T(A - bk^T) = C^T\lambda_4 \tag{3.8}$$

Equation (3.8) can be rewritten as

$$C^T(A-\lambda_4 I)=C^T bk^T \tag{3.9}$$

The equation (3.4) with sliding surface (3.7) can be transformed into reduced order system.

It is assumed that values $\lambda_1,\lambda_2,\lambda_3$ are the desired eigenvalues of A while λ_4 is an arbitrary values do not belong to the spectrum of A in the system (3.4) with sliding surface. That is, $\det(A-\lambda_4 I)\neq 0$.

By controllability of (A,b), there exist $C^T b\neq 0$ and $(A-\lambda_4 I)^{-1}$ because λ_4 is not an eigenvalue of A.

Now, C^T is defined as follows:

$$C^T = h^T P_1(A) \tag{3.10}$$

$$P_1(\lambda)=(\lambda-\lambda_1)(\lambda-\lambda_2)(\lambda-\lambda_3)\equiv p_1+p_2\lambda+p_3\lambda^2+\lambda^3$$

$$C^T b=1$$

where $P_1(\lambda)$ is characteristic polynomial of system (3.4) with sliding surface (3.7).

Proof:

From equation (3.5) and (3.10), the following can be obtained.

$$P_1(A)b = p_1 b + p_2 Ab + p_3 A^2 b + A^3 b$$

$$=\begin{bmatrix} b & Ab & A^2 b & A^3 b\end{bmatrix}\begin{bmatrix} p_1 & p_2 & p_3 & 1\end{bmatrix}^T$$

$$C^T b = h^T P_1(A)b = [0,0,0,1]\left[b, Ab, A^2 b, A^3 b\right]^{-1}\begin{bmatrix} b & Ab & A^2 b & A^3 b\end{bmatrix}\begin{bmatrix} p_1 & p_2 & p_3 & 1\end{bmatrix}^T = 1.$$

From equations (3.5), (3.9) and (3.10), the following can be obtained.

$$k^T = h^T P(A) = C^T (A - \lambda_4 I) = h^T P_1(A)(A - \lambda_4 I) \tag{3.11}$$

From equation (3.11), $P(\lambda)$ in equation (3.5) can be rewritten as

$$P(\lambda) = P_1(\lambda)(\lambda - \lambda_4)$$

ii) Dynamic Controller

Using equations (3.2) and (3.5), equation (3.1) can be transformed into

$$\dot{x} = (A - bk^T)x + bu_1 \tag{3.12}$$

where u_1 is dynamic controller acted as perturbation of system input u.

A new variable z is defined as

$$z = \begin{bmatrix} x^1 \\ \cdots \\ S \end{bmatrix} = \begin{bmatrix} I & 0 \\ \cdots & \\ C^T & \end{bmatrix} x = Tx \tag{3.13}$$

where $x^1 = [x_1, x_2, x_3]^T$ is the first three state variables of x acted as the state variable of reduced system and $S = C^T x$ becomes the last state variable of z, and there exists T^{-1}.

From $x = T^{-1}z$, equation (3.12) can be expressed as

$$\dot{z} = T(A - bk^T)T^{-1}z + Tbu_1 = \bar{A}z + \bar{B}u_1 \tag{3.14}$$

For 4x4 matrix T to be invertible, the last component of C^T must be nonzero. Since these vectors are nonzero, the condition can always be satisfied by reordering the components of the state vector x.

The transformed system equation (3.14) under the above conditions is

$$\dot{x}^1 = A_1 x^1 + a_1 S + b^1 u_1 \tag{3.15}$$

$$\dot{S} = \lambda_4 S + u_1 \tag{3.16}$$

where

$$\bar{A} = T(A - bk^T)T^{-1} = \begin{bmatrix} A_1 & a_1 \\ 0 & \lambda_4 \end{bmatrix},\ \bar{B} = Tb = \begin{bmatrix} b^1 \\ 1 \end{bmatrix},\ b^1 = [b_1, b_2, b_3]^T,$$

$$k^T = [k_1 \quad k_2 \quad k_3 \quad k_4]$$

$$A_1 = \begin{bmatrix} (a_{11} - b_1 k_1) - \dfrac{(a_{14} - b_1 k_4)c_1}{c_4} & (a_{12} - b_1 k_2) - \dfrac{(a_{14} - b_1 k_4)c_2}{c_4} & (a_{13} - b_1 k_3) - \dfrac{(a_{14} - b_1 k_4)c_3}{c_4} \\ (a_{21} - b_2 k_1) - \dfrac{(a_{24} - b_2 k_4)c_1}{c_4} & (a_{22} - b_2 k_2) - \dfrac{(a_{24} - b_2 k_4)c_2}{c_4} & (a_{23} - b_2 k_3) - \dfrac{(a_{24} - b_2 k_4)c_3}{c_4} \\ (a_{31} - b_3 k_1) - \dfrac{(a_{34} - b_3 k_4)c_1}{c_4} & (a_{32} - b_3 k_1) - \dfrac{(a_{34} - b_3 k_4)c_2}{c_4} & (a_{33} - b_3 k_3) - \dfrac{(a_{34} - b_3 k_4)c_3}{c_4} \end{bmatrix}$$

$$a_1 = \begin{bmatrix} \dfrac{a_{14} - b_1 k_4}{c_4} & \dfrac{a_{24} - b_2 k_4}{c_4} & \dfrac{a_{34} - b_3 k_4}{c_4} \end{bmatrix}^T$$

Proof:

The proof of equation (3.15) is shown in Appendix.

From equations (3.7), (3.8), (3.10) and (3.12), the derivative of sliding surface is obtained as

$$\dot{S} = C^T \dot{x} = C^T \left[\left(A - bk^T \right) x + bu_1 \right] = C^T \left(A - bk^T \right) x + C^T b u_1$$
$$= \lambda_4 C^T x + u_1 = \lambda_4 S + u_1$$

The spectrum of the matrix A_1 consists of the desired eigenvalues $\lambda_1, \lambda_2, \lambda_3$.

In $S = 0$ and $\dot{S} = 0$, equation (3.15) results in the following motion equation.

$$\dot{x}^1 = A_1 x^1 \tag{3.17}$$

The dynamic controller u_1 is designed to enforce a sliding mode in the sliding surface $S = 0$ such that $\lim_{S \to 0} S\dot{S} < 0$.

$$u_1 = -M(x,t)sign(S) \tag{3.18}$$

where $M(x,t) > \left|\lambda_4 C^T x\right|$.

Proof:

From equations (3.16) and (3.18), the followings must be obtained to stabilize the dynamic system.

i) $S > 0$ and $\dot{S} < 0$

$$\dot{S} = \lambda_4 C^T x + u_1 < 0$$

$$u_1 < -\lambda_4 C^T x$$

$$-M(x,t)sign(S) < -\lambda_4 C^T x$$

$$M(x,t) > \lambda_4 C^T x \tag{3.19}$$

ii) $S < 0$ and $\dot{S} > 0$

$$\dot{S} = \lambda_4 C^T x + u_1 > 0$$

$$u_1 > -\lambda_4 C^T x$$

$$-M(x,t)sign(S) > -\lambda_4 C^T x$$

$$M(x,t) < -\lambda_4 C^T x \tag{3.20}$$

From (3.19) and (3.20), the following condition is obtained to satisfy $\lim_{S\to 0} S\dot{S} < 0$.

$$M(x,t) > \left|\lambda_4 C^T x\right| \tag{3.21}$$

If the control may take only two extreme values $+M_0$ or $-M_0$, then equation (3.18) with $M\left(x,t\right) = M_0$ forces a sliding mode to converge to the sliding surface $S = 0$ governed by (3.16) as well. Fig. 3.1 shows the block diagram of the proposed controller.

The sliding mode control causes chattering when it is implemented in computers for the finite sample frequency. In order to suppress the chattering, a saturation function is used instead of a signum function.

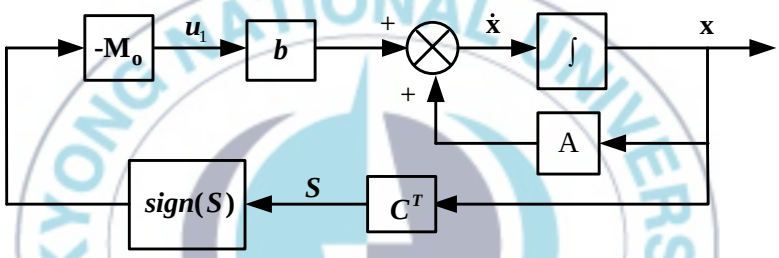

Fig. 3.1 Block Diagram of the Controller

4

Hardware Design and Implementation

4.1 Overall Control System

The mobile inverted pendulum is built to test out the performance of controller in stabilizing an unstable system.

For the control system, a PIC-based controller was developed [25]. The controller is composed of two parts: servo controller and main controller. The configuration diagram of the overall control system is shown in Fig. 4.1. In the diagram, two PIC16F877 microcontrollers are integrated into one module for two motors of the left and the right wheels. The motors are driven via LMD18200 Dual Full Bridge Drivers. This module implements Lyapunov-based velocity control using feedback from an optical encoder attached to the motors. One PIC16F877 microcontroller is used as master, and receives the signal from sensors, render the control law and send velocity command to the servo controller. The servo controller is responsible for reaching and maintaining the speed. The master communicates to the motor drivers via I2C. With the modular structure, the control system can manage a control law with a sampling time of $10\,ms$, even $5\,ms$ in some critical applications. A configuration for sensors is developed to obtain the system states and realize the above controllers, including one tilt sensor and two incremental encoders. The tilt sensor measures the angle of inverted pendulum. The incremental encoders mounted on the cart are utilized measure the speed of the wheels. The position and speed of the cart on a straight line can be also determined from the speed of rotation of two wheels. These measurements can then be fed back to the controllers to impose the desired closed loop dynamics. The implementation of the PIC-based control system including servo controller and main controller is shown in Fig. 4.2.

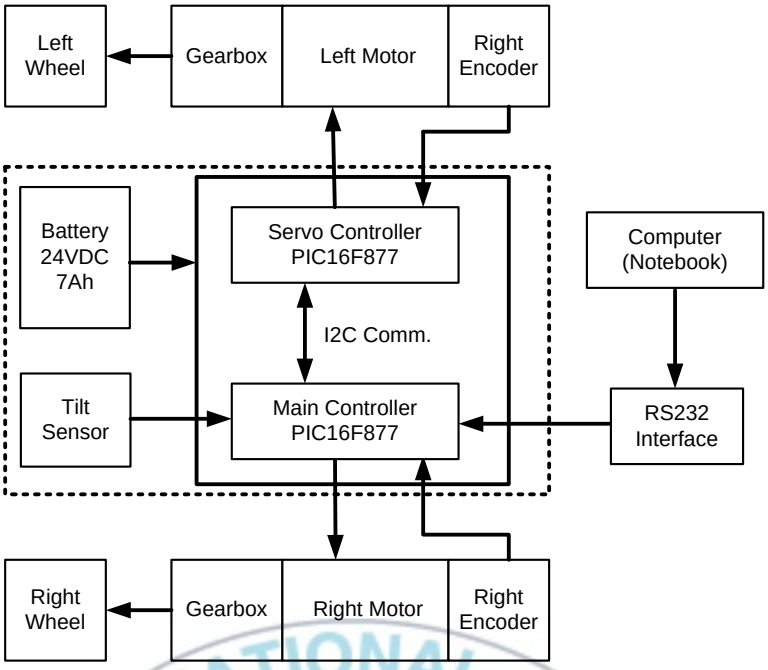

Fig. 4.1 Configuration of the Control System

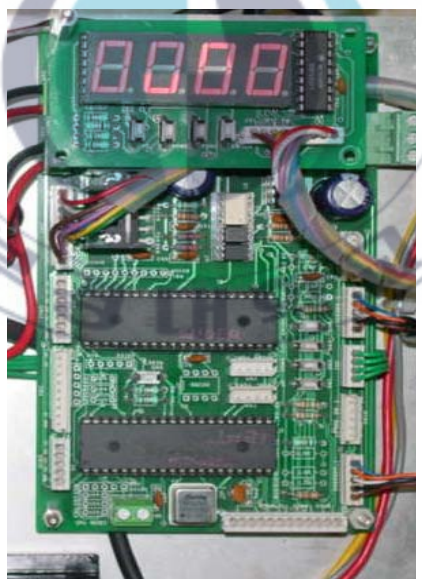

Fig. 4.2 PIC-based Control System

4.2 Tilt Sensor

Tilt sensor provides a precise measurement of the pitch angle as shown in Fig. 4.3 and 4.4. Fig. 4.5 shows relation between output voltage of the sensor and pendulum angle.

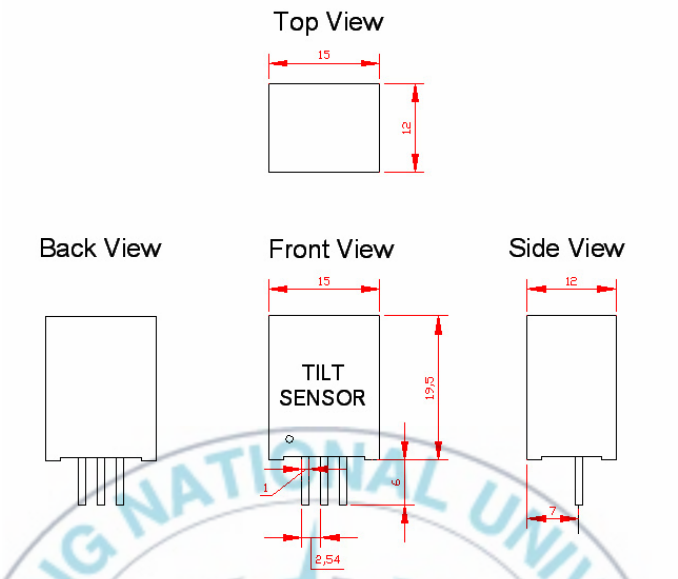

Fig. 4.3 Dimension of Tilt Sensor

Fig. 4.4 Tilt Sensor

The main specifications are summarized as following:

● Measuring range: ±60^{o}

- Resolution: $< 0.1^{o}$
- Transverse sensitivity: $< 0.5\%$
- Response time: < 0.5 second
- Sensitivity: approx 30 mV/degree

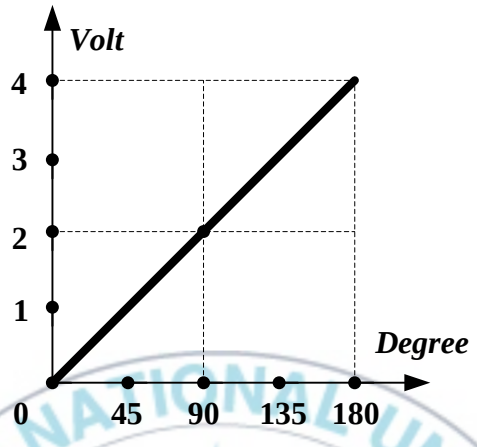

Fig. 4.5 Tilt Sensor Voltage Output

4.3 Motor Control

To control the speed of a DC motor, a variable voltage DC power source is needed. If the DC motor is powered on by a switch, the motor do not respond immediately, that is, it takes a small time to reach full speed. Similarly, if the power is switched off sometime before the motor reaches full speed, the motor starts to slow down. So, if the power is switched on and off quickly enough, the motor runs on some speed between zero and full speed. To control the motor speed, the width of the pulses varies Pulse Width Modulation. The current supplied for motor can be got by the PIC16F877 through the current sense of LMD18200 as shown in Fig. 4.6.

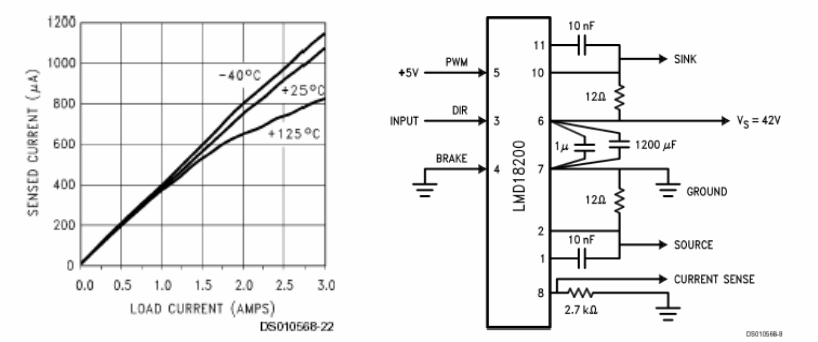

Fig. 4.6 Sensed Current Output of LMD18200

To perform indirect closed loop velocity control, an optical incremental encoder as shown in Fig. 4.7 is utilized to measure the speed of the wheel. Incremental encoders typically consist of a light source, a rotating pattern disc, a stationary detector, and processing electronics to convert the analog detector signal to a digital output as shown in Fig. 4.8. This type of encoder has two channels, which output digital square waves proportional to the number of windows on the optical code disc. The output of the encoder is a square wave whose frequency is proportional to the angular velocity of the wheels. The typical wave form of output is presented in Fig. 4.9.

Fig. 4.7 Typical Incremental Encoder

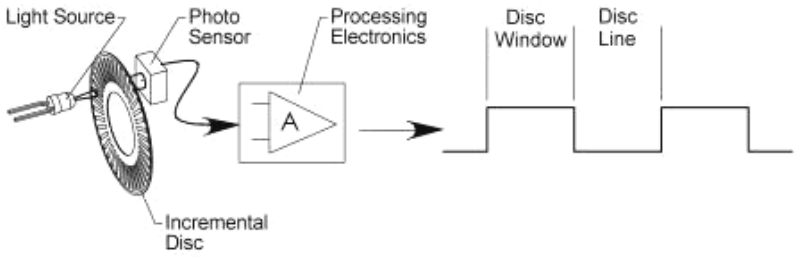

Fig. 4.8 Components of an Incremental Encoder

Incremental square waves are counted by a controller to determine wheel position, velocity and acceleration. Additionally, by observing the phase sequence between the two digital output channels, a controller can determine the direction of wheel rotation.

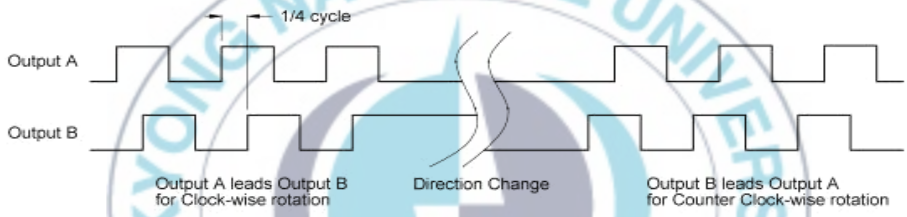

Fig. 4.9 Output Wave Form of an Encoder

A signal per rotation is often found on a third channel of incremental encoders and is commonly called the index or reference pulse as shown in Fig. 4.10. This signal is typically used to mark a particular location in a system's rotation that obtains mechanical location often called a home position. The drawback to an incremental encoder is that if the controller's counter should happen to lose power or miscount, the system must be cycled back to a known location such as an index location before restarting. An absolute encoder is used instead of an incremental

encoder in order to overcome the cost, inconvenience and potential frequency of a home cycle restart sequence. In this application, the index pulse is not used.

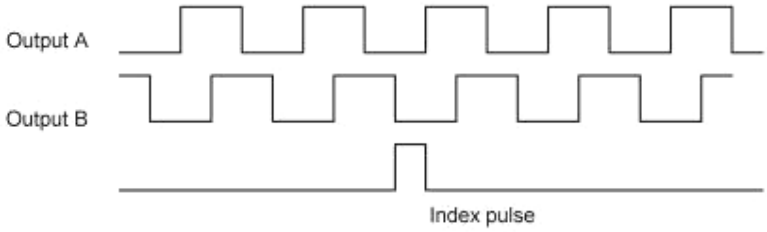

Fig. 4.10 Incremental Encoder: Two Channels and Index Pulse

Motor controller using PIC16F877 performs a closed loop velocity control. The angular velocity is calculated as the following equation:

$$S = \frac{Counts / P}{T} \times 60 \tag{4.1}$$

where

S : angular velocity of motor (rpm)

$Counts$: number of pulses counted during the sampling time of T

P : number of pulses per one revolution of encoder

T : sampling time, sec

The motor driver uses pin *RC2* for PWM generation and pin *RC1* for capturing pulse from encoder. Motor controller counts the rising edges for a period of time to produce real angular velocity of the wheel. The master is

configured to send the desired angular velocity command to the servo controller. The controller, in turn, compares the values received from the master to the real one. If the real velocity is lower than the desired angular velocity, the velocity must be increased and vice versa. The behavior for the motor to speed up and down is performed using Lyapunov function.

Velocity Control Using Lyapunov Function

First, the following relationship has to be set up:

$$\omega = KV \tag{4.2}$$

where

ω : real angular velocity of the motor.

K : characteristic constant of the motor, and it is achieved by experiment.

V : average voltage applied to the motor.

The experiment gives $K = 274$ for this case.

$$\dot{\omega} = Ku \text{ where } u = \dot{V} \tag{4.3}$$

Angular velocity error is defined as

$$\varepsilon = \omega - \omega_r \tag{4.4}$$

The time derivative of ε is

$$\begin{aligned}\dot{\varepsilon} &= \dot{\omega} - \dot{\omega}_r \\ &= Ku - \dot{\omega}_r\end{aligned} \tag{4.5}$$

where K is positive value and ω_r is reference angular velocity of the motor.

Lyapunov function W is defined as

$$W = \frac{1}{2}\varepsilon^2 > 0 \tag{4.6}$$

Using equations (4.4) and (4.5), the derivative of W is obtained as

$$\dot{W} = \varepsilon\dot{\varepsilon} = \varepsilon(Ku - \dot{\omega}_r) \tag{4.7}$$

For $\dot{W}$ to be negative, the following can be chosen

$$Ku - \dot{\omega}_r = -K_1\varepsilon \tag{4.8}$$

$$\dot{\varepsilon} = -K_1\varepsilon \le 0 \tag{4.9}$$

where K_1 is positive value.

Using equation (4.9), (4.7) is given as

$$\dot{W} = \varepsilon\dot{\varepsilon} = -K_1\varepsilon^2 \le 0 \tag{4.10}$$

From (4.6) and (4.10), ε goes to zero as $t \to \infty$ by Barbalat Lemma. That is, the velocity control is asymptotically stable.

From (4.3) and (4.8), the following is obtained

$$\dot{V} = u = \frac{-K_1 \varepsilon + \dot{\omega}_r}{K} \tag{4.11}$$

The duty of the PWM signal can be derived from V , the voltage applied to the motor.

4.4 Microcontroller

The PIC16F877 is a 40-pin, high performance RISC (Reduced Instruction Set Computer) microcontroller in Fig. 4. 11. The main specifications are summarized as following:

- FLASH program memory: 8Kx14bit words
- Data Memory (RAM):368x8bytes
- EEPROM Data Memory: 256x8bytes
- Interrupts: 14 sources
- Timer 0: 8-bit timer/counter with 8-bit prescaler
- Timer 1: 16-bit timer/counter with prescaler, can be incremented during SLEEP via external crystal/clock
- Timer 2: 8-bit timer/counter with 8-bit period register, prescaler and postscaler
- Two Capture/Compare/PWM modules
- Capture is 16-bit, max resolution is 12.5ns
- Compare is 16-bit, max resolution 200 ns

- PWM max. resolution 10 bit
- 10-bit multi-channel Analog-to-Digital converter
- Synchronous Serious Port (SSP) with SPI Master Mode and I2C (Master/Slave)
- Universal Synchronous Asynchronous Receiver Transmitter (USART/SCI) with 9-bit address detection
- Parallel Slave Port (PSP) 8-bit wide with external $\overline{RD}$, $\overline{WR}$ and $\overline{CS}$ controls
- Power saving SLEEP mode
- In-Circuit Serial Programming (ICSP) via two pins

The master has the function of rendering the control law. The linear and angular velocities which are derived from the control law, used to transfer to the servo controller via I2C.

With the functions on PIC16F877 above, the controller and user interface were designed, and its schematic diagram are shown in Fig. 4.12.

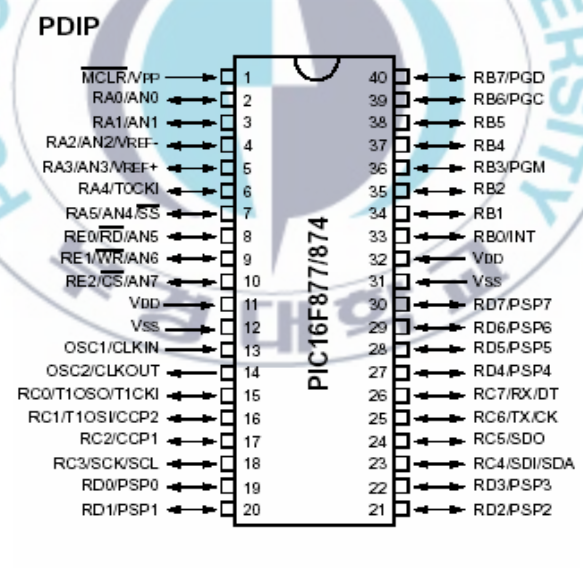

Fig. 4.11 Pin Diagram of PIC16F877

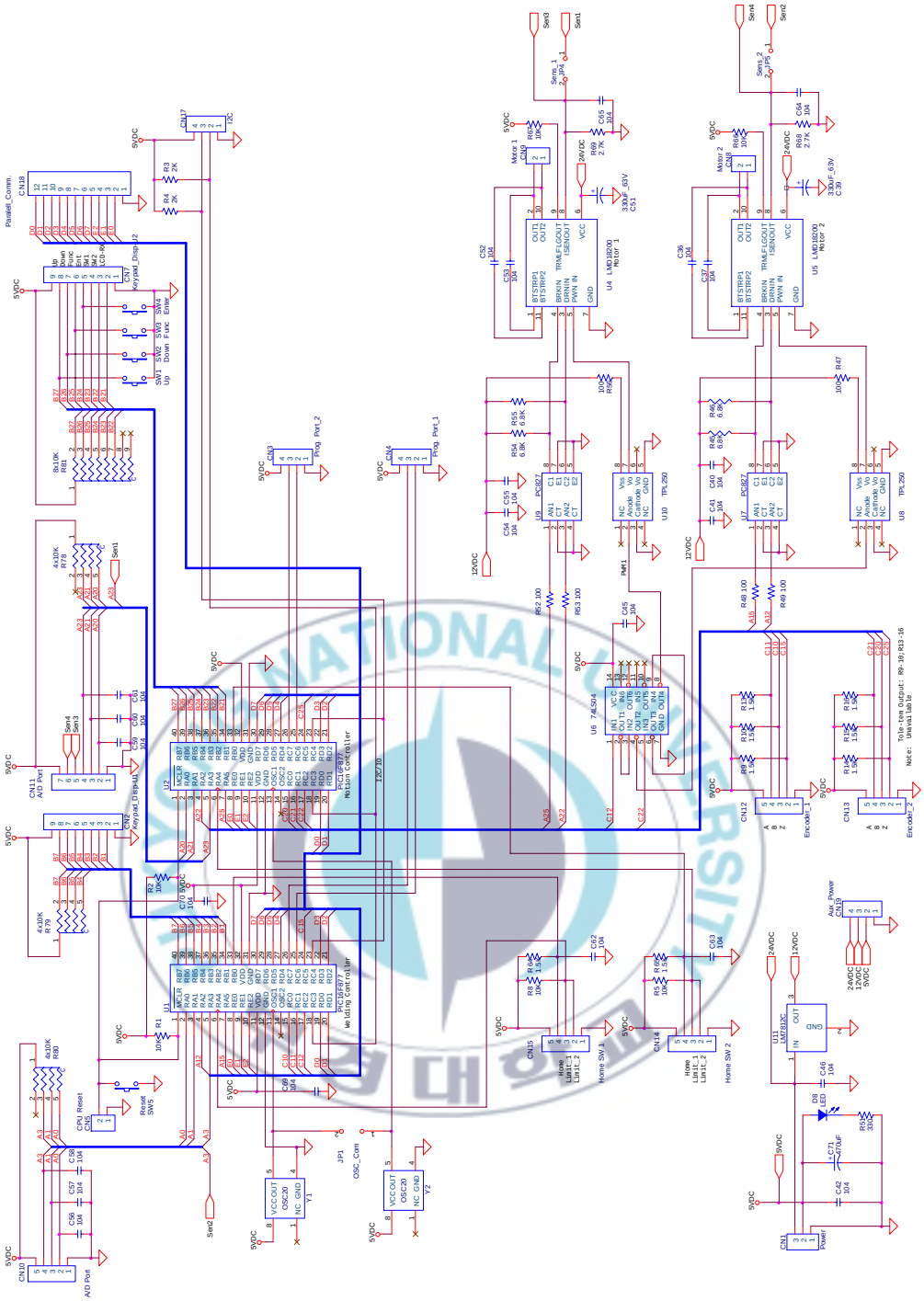

Fig. 4.12 Schematic Diagram

5

Simulation and Experimental Results

In this chapter, simulations and experiments are done to prove the effectiveness of the stabilizing controller. The parameters and initial values for the simulation and experiment are given in Table 5.1.

Table 5.1 Numerical Values for the Simulation

Parameter	Description	Value	Unit
Mobile inverted pendulum parameters			
r	Radius of the wheel	0.05	m
M_p	Mass of the inverted pendulum	1.13	Kg
I_p	Moment of inertia of pendulum around z axis	0.004	$Kg \cdot m^2$
K_m	Torque constant of motor	0.006	Nm / A
R	Nominal terminal resistance	3	Ω
M_w	Mass of the wheel	0.03	Kg
I_w	Moment of inertia of the wheel	0.001	$Kg \cdot m^2$
L	Distance between the wheel's center and the pendulum's center of gravity	0.07	m
K_e	Back electromotive force voltage constant	0.007	$V \sec / rad$
g	Gravitational acceleration	9.8	$m / \sec^2$

Then equation (2.36) becomes

$$\begin{bmatrix} \dot{x}_r \\ \ddot{x}_r \\ \dot{\phi} \\ \ddot{\phi} \end{bmatrix} = \begin{bmatrix} 0 & 1 & 0 & 0 \\ 0 & -0.0097 & 11.1594 & 0 \\ 0 & 0 & 0 & 1 \\ 0 & -0.0293 & 172.1160 & 0 \end{bmatrix} \begin{bmatrix} x_r \\ \dot{x}_r \\ \phi \\ \dot{\phi} \end{bmatrix} + \begin{bmatrix} 0 \\ 0.0815 \\ 0 \\ 0.2456 \end{bmatrix} V \qquad (5.1)$$

The controllability matrix of (5.1) is as follows:

$$\Gamma = \begin{bmatrix} b \\ Ab \\ A^2b \\ A^3b \end{bmatrix}^T = \begin{bmatrix} 0 & 0.0815 & -0.0008 & 2.7408 \\ 0.0815 & -0.0008 & 2.7408 & -0.0532 \\ 0 & 0.2456 & -0.0024 & 42.2717 \\ 0.2456 & -0.0024 & 42.2717 & -0.4913 \end{bmatrix} \qquad (5.2)$$

It is readily shown that the rank of matrix is 4.

5.1 Control Problem

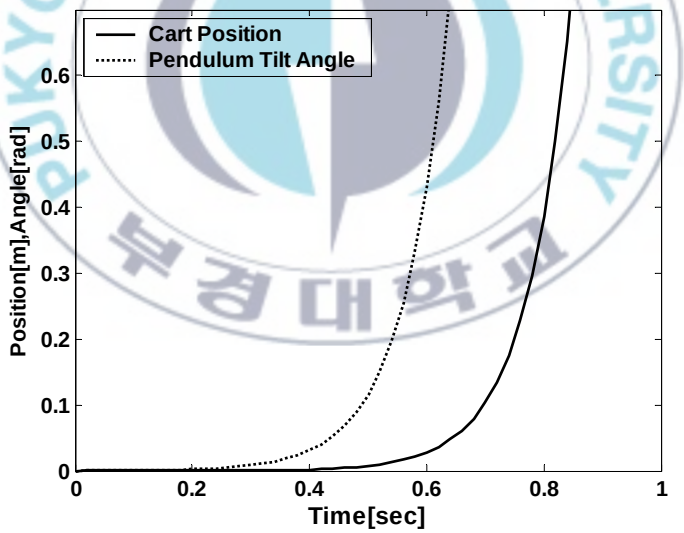

Fig. 5.1 Open Loop Impulse Response

Because the mobile inverted pendulum system is inherently unstable, an impulse input applied to the open loop system causes the tilt angle and position of the system to rise unboundedly. Fig. 5.1 shows the simulation when an impulse input is applied to the uncontrolled system.

5.2 Simulation and Experimental Results of Stabilizing Controller

The experimental mobile inverted pendulum used for this thesis is shown in Fig. 5.2.

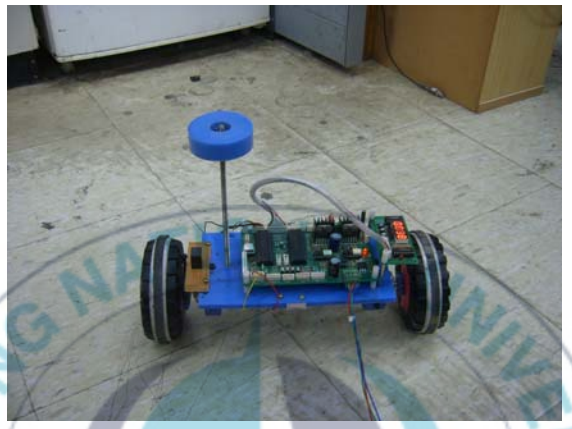

Fig. 5.2 Experimental Mobile Inverted Pendulum

The designed parameters of the sliding surface are $\lambda_1 = -1, \lambda_2 = -1, \lambda_3 = -3$; and the positive constant of the control law u_1 is $M_0 = 40$. The initial values are $x_r = 0.5m$ and $\varphi = 0.3rad$.

The objective of this controller is to make the state variable of the system converge to zero at the shortest time possible. Simulation and experimental results are shown as follows. Fig. 5.3 shows that the simulation result of cart position x_r is bounded around zero after five seconds. Fig. 5.4 presents the simulation result of the wheel angular velocity ω is within $\pm 1.5rad/sec$. Fig. 5.5 shows the wheel angular velocity in the experiment. Fig. 5.6 presents the relation between motor angular velocity and output voltage of wheel motor. Figs. 5.7 and 5.8 show the

inverted pendulum angle in simulation and experiment, respectively. The pendulum angle in simulation represents a small angle from the vertical upward direction, and Fig. 5.7 presents that φ is stable after three seconds. But Fig. 5.8 shows the experimental pendulum angle $\varphi_1 = \frac{\pi}{2} + \varphi$ measured from the horizontal direction to the vertical direction by sensors. Fig. 5.9 shows the relation between φ_1 and output voltage of tilt sensor. Fig. 5.10 presents the simulation result of the pendulum angular velocity $\dot{\varphi}$ is within $\pm 0.05 rad/sec$. Fig. 5.11 shows the simulation evolution of the system input u_1. Fig. 5.12 presents PWM output of controller with corresponding to control input u . Fig. 5.13 shows the sliding surface and convergence to zero within one second.

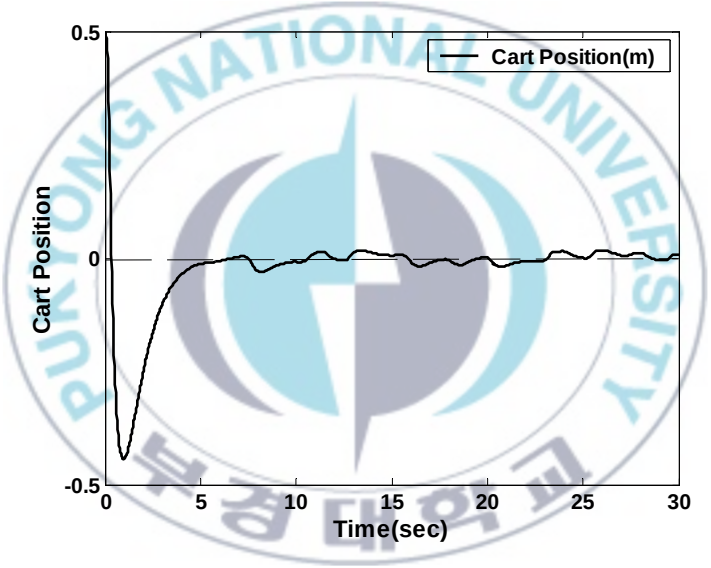

Fig. 5.3 Cart Position x_r

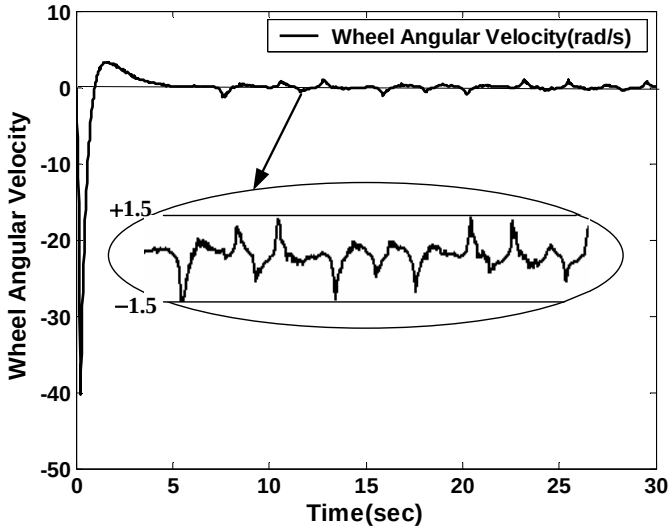

Fig. 5.4 Wheel Angular Velocity

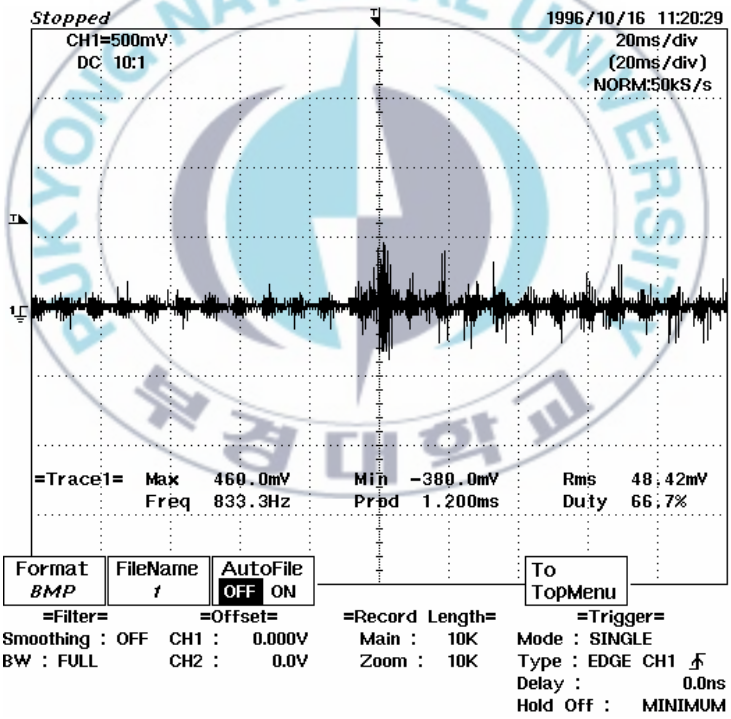

Fig. 5.5 Experimental Wheel Angular Velocity

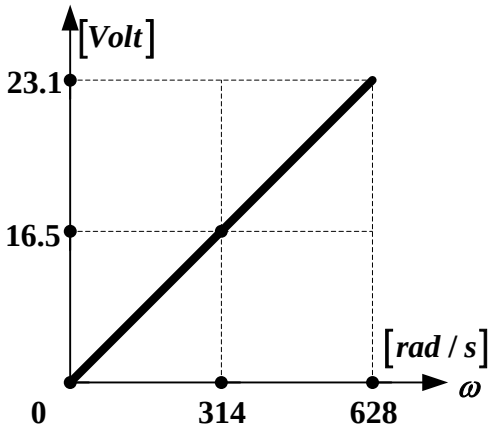

Fig. 5.6 Relation between Motor Angular Velocity ω and Output Voltage of Wheel Motor

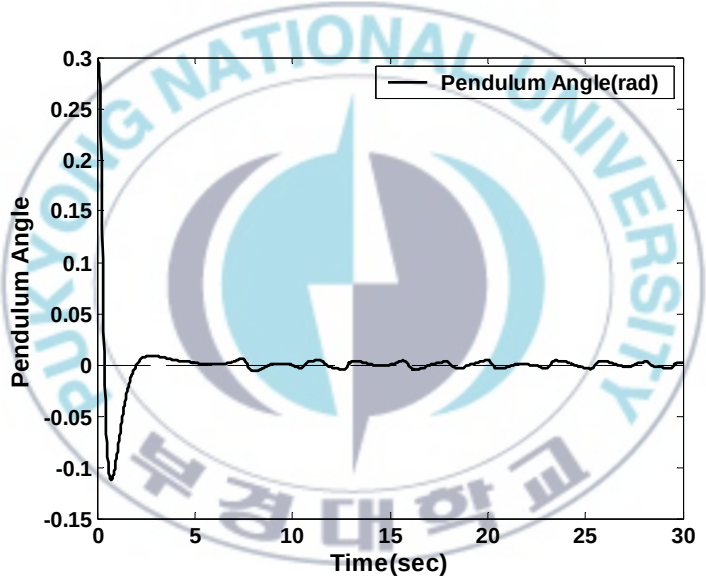

Fig. 5.7 Pendulum Angle φ

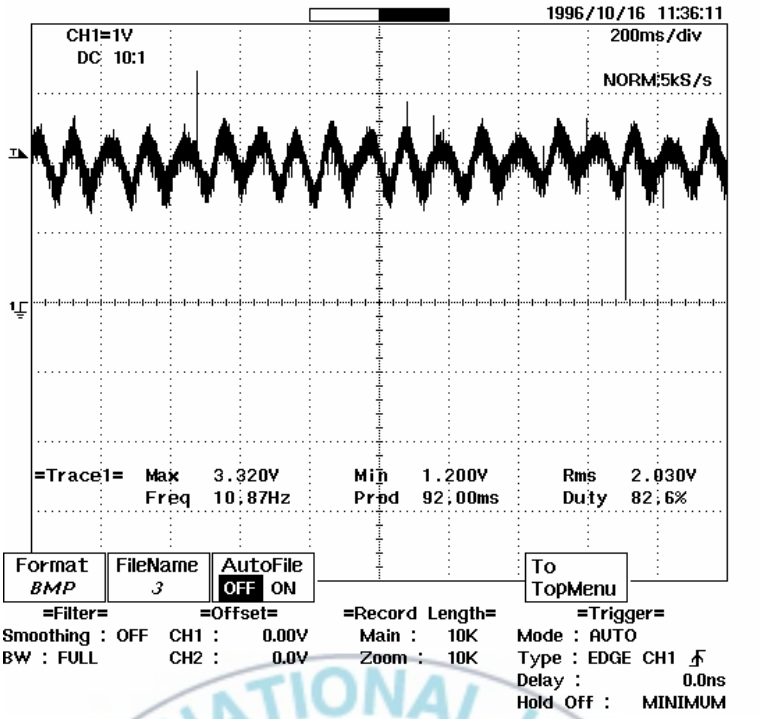

Fig. 5.8 Experimental Pendulum Angle

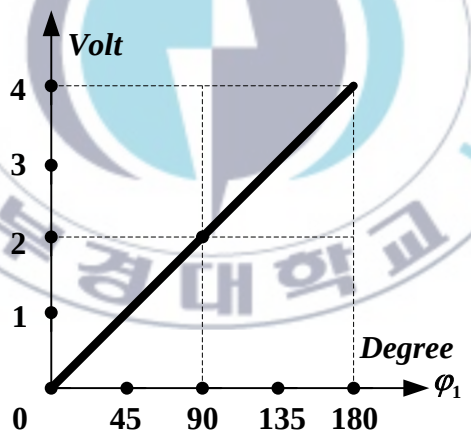

Fig. 5.9 Relation between φ_1 and Output Voltage of Tilt Sensor

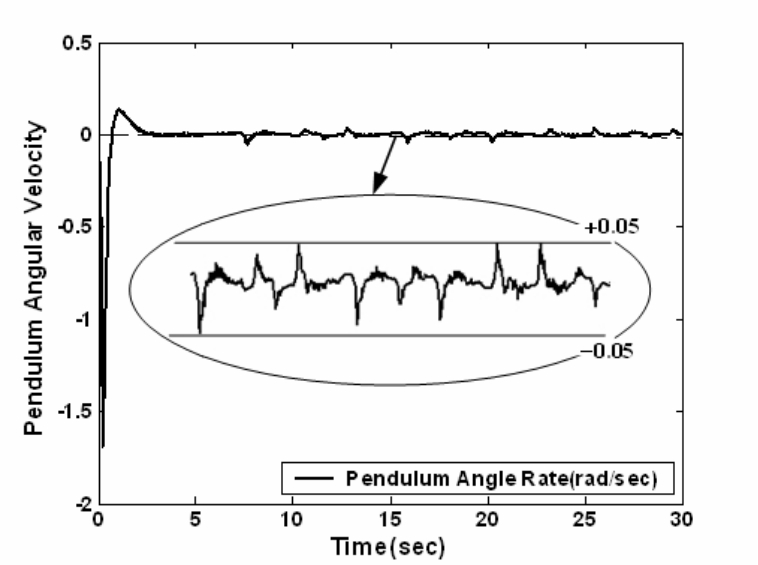

Fig. 5.10 Pendulum Angular Velocity $\dot{\varphi}$

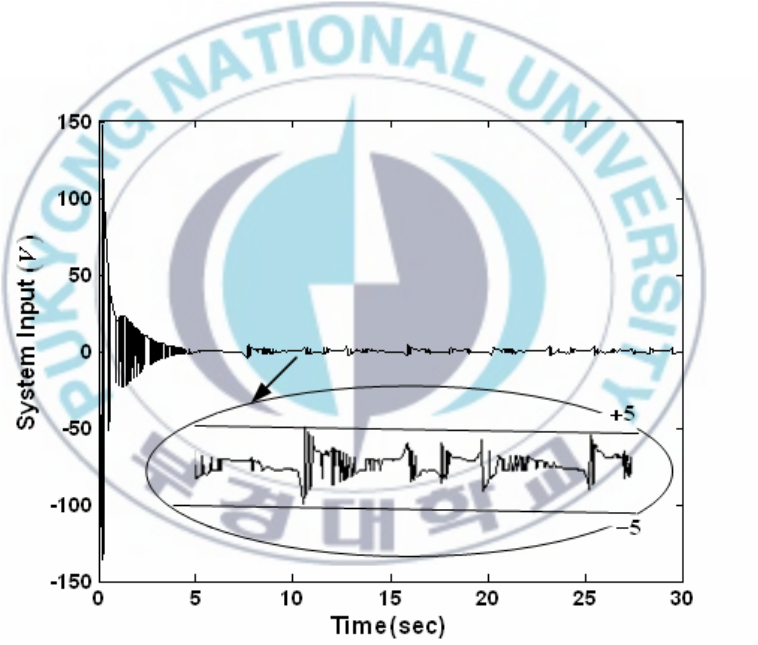

Fig. 5.11 System Input u_1

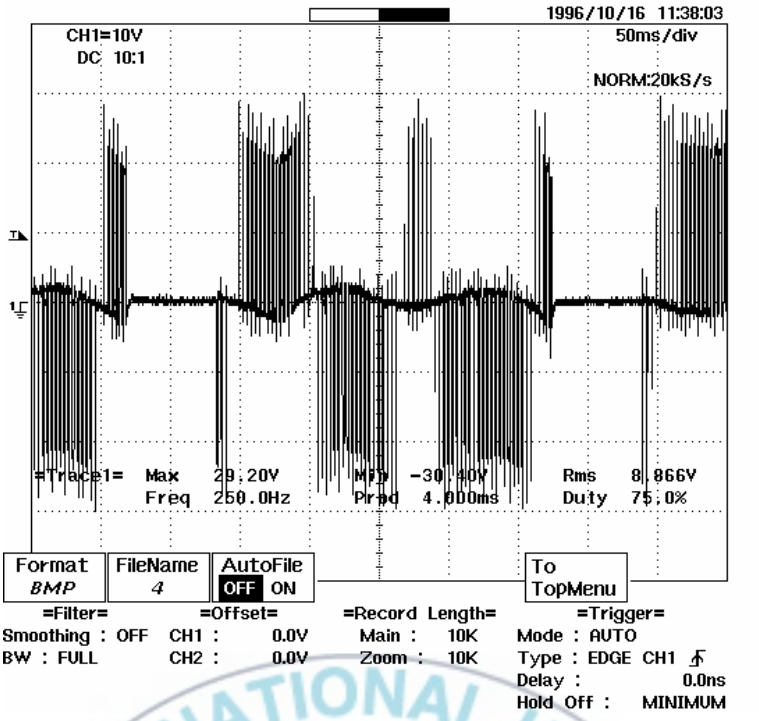

Fig. 5.12 PWM Output of Controller with Corresponding to Control Input u

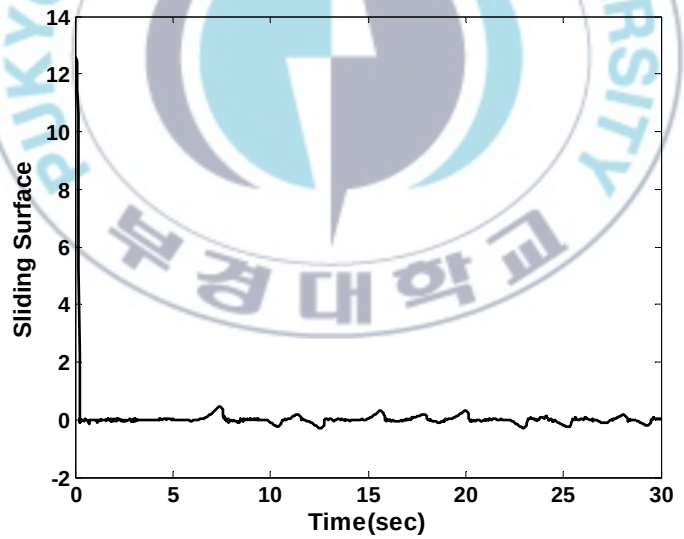

Fig. 5.13 Sliding Surface S

5.3 Summary

This section is summarized as follows:

- The stabilizing controller via sliding mode control can be used to stabilize the mobile inverted pendulum from the simulation and experimental results.

6

Conclusions and Future Works

6.1 Conclusions

This thesis presents controllers design to stabilize the mobile inverted pendulum. The mobile inverted pendulum is a system with an inverted pendulum attached to a mobile cart with two coaxial wheels. In this thesis, the conclusions are given as the following:

- The dynamic equation of the mobile inverted pendulum is established.
- To control the system, the controller via sliding mode control is applied to stabilize the mobile inverted pendulum.
- To implement the controllers for the mobile inverted pendulum, the hardware which is the integration of three PIC16F877 microprocessors is developed. Tilt sensor and two incremental encoders are utilized to obtain the system states and realize the proposed controller.
- The simulation and experimental results are shown to prove the effectiveness of the proposed model and controller.

6.2 Future Works

There are some works that will be considered as future works in the scope of this thesis:

- Consideration in the nonlinear system via backstepping method.
- Control of this model to track arbitrary reference.
- Consideration of uneven terrain conditions.

References

[1] F. Grasser, A. D. Arrigo, S. Colombi and A. C. Rufer, “JOE: A Mobile, Inverted Pendulum”, *IEEE Trans. Indus. Elec.*, Vol. 49, No. 1, 107-114, Feb. 2002.

[2] V. Williams and K. Matsuoka, “Learning to Balance the Inverted Pendulum Using Neural Networks”, *IEEE Conference on Neural Networks*, Vol. 1, pp. 214-219, 2002.

[3] R. J. Lee, K. C. Chou, S. H. Liu and J. Y. Yen, “Solid Modeling Based Servo System Design for a High Speed Micro Grinding Machine”, *Machine Tools & Manufacture,* Vol. 46, pp.208-217, 2006.

[4] F. Esfandiari and H. K. Khalil, “Output Feedback Stabilization of Fully Control System”, *International Journal of Control*, Vol. 56, pp. 1007-1037, 1992.

[5] R. J. Wai and L. J. Chang, “Adaptive Stabilizing and Tracking Control for a Nonlinear Inverted-Pendulum System via Sliding-Mode Technique”, *IEEE Trans. Indus. Elec.*, Vol. 53, No. 2, Apr. 2006.

[6] R. N. Gasimov, A. Karamancioglu and A. Yazici, “A Nonlinear Programming Approach for the Sliding Mode Control Design”, *Applied Mathematical Modeling*, Vol. 29, pp. 1135-1148, 2005.

[7] C. Edwards, “A Practical Method for the Design of Sliding Mode Controllers Using Linear Matrix Inequalities”, *Automatica,* Vol. 40, pp. 1761-1769, 2004.

[8] J. H. Wu, D. L. Pu and H. Ding, “Adaptive Robust Motion Control of SISO Nonlinear Systems with Implementation on Linear Motors”, *Mechatronics,* 2007.

[9] R. J. Lee, K. C. Chou, S. H. Liu and J. Y. Yen, “Solid Modeling Based Servo System Design for a High Speed Micro Grinding Machine”, *Machine Tools & Manufacture*, Vol. 46, pp. 208-217, 2006.

[10] C. Bonivento, L. Marconi and R. Zanasi, “Output Regulation of Nonlinear System by Sliding Mode”, *Automatica*, Vol. 37, pp. 535-542, 2001.

[11] J. J. E. Slotine, J. K. Hedrick and E. A. Misawa, “On Sliding Observer for Nonlinear System”, *Journal of Dynamics System, Measurement and Control*, Vol. 109, pp. 245-252, 1987.

[12] R. Sreedhar, B. Fernandez and J. Y. Masawa, “Robust Fault Detection in Nonlinear System Using Sliding Mode Observer”, *Proceedings of IEEE Conference on Control and Applications*, Vol. 2, pp. 715-721, Sept. 1993.

[13] Y. Yao and M. Tomizuka, “Adaptive and Robust Control of Robot Manipulators: Theory and Comparative Experiment”, *Proceedings IEEE Conference on Decision and Control*, pp. 1290-1295, 1994.

[14] Y. Huang and J. Han, “Analysis and Design for Nonlinear Continuous Extended State Observer”, *Chinese Science Bulletin*, pp. 1373-1379, 2000.

[15] Z. Gao, S. Hu and F. Jiang, “A Novel Motion Control Design Approach Based on Active Disturbance Projection”, *Proceedings the 40th IEEE Conference on Decision and Control*, Vol. 5, pp. 4877-4882, Dec. 2001.

[16] Z. Gao, Y. Huang and J. Han, “An Alternative Paradigm for Control System Design”, *Proceedings the 40th IEEE Conference on Decision and Control*, Orlando, Florida USA, Vol. 5, pp. 4578-4585, Dec. 2001.

[17] J. Han, “Auto-Disturbance-Rejection Control and Its Application”, *Control and Decision*, Vol. 13, No. 1, pp. 19-23, 1998.

[18] J. Ackermann and V. Utkin, “Sliding Mode Control Design Based on Ackermann’s Formula”, *IEEE Trans. Auto. Con.*, Vol.43, No.2, 234-237, Feb. 1998.

[19] P. J. McKerrow, *Introduction to Robotics*, Addivision Wesley Longman China Ltd., VVP, 1998.

[20] G. F. Franklin, J. D. Powell and A. Emami-Naeini, *Feedback Control of Dynamic Systems*, London: Prentice Hall, Inc., New Jersey, 2002.

[21] J. J. E. Slotine and W. Li, *Applied Nonlinear Control*, New Jersey: Prentice-Hall International, Inc., Englewood Cliffs, 1991.

[22] D. Necsulescu, *Mechatronics*, Prentice Hall, 2002.

[23] V. I. Utkin, *Sliding-modes in Control Optimization*, Springer-Verlag, 1992.

[24] C. Edwards and S. K. Spurgeon, *Sliding Mode Control: Theory and Applications*, Taylor & Francis, Mar. 1998.

[25] T. L. Chung, *A Nonlinear Feedback Control of Wall-Following Mobile Robot*, Master Thesis, The Graduate School of Pukyong National University, Feb. 2004.

Publications and Conferences

A. Publication

[1] Ming Tao Kang, Nguyen Thanh Phuong, Hak Kyeong Kim and Sang Bong Kim, “Stabilizing Control for Nonlinear Mobile Inverted Pendulum via Sliding Mode Technique”, *Mechatronics*, July 2007, submitted.

B. Conference

[1] Ming Tao Kang, Hoang Duy Vo, Hak Kyeong Kim and Sang Bong Kim, “Control System Design for a Mobile Inverted Pendulum via Sliding Mode Technique”, *The IEEE International Conference on Mechatronics*, Kumamoto City, Japan, May 2007.

[2] Ming Tao Kang, Hak Kyeong Kim, Yeon Wook Choe and Sang Bong Kim, “Sliding Mode Control for Mobile Inverted Pendulum”, *International Symposium on Mechatronics and Automatic Control*, Hochiminh City, VietNam, October 2007, submitted.

Appendix

$$A - bk^T = \begin{bmatrix} a_{11} & a_{12} & a_{13} & a_{14} \\ a_{21} & a_{22} & a_{23} & a_{24} \\ a_{31} & a_{32} & a_{33} & a_{34} \\ a_{41} & a_{42} & a_{43} & a_{44} \end{bmatrix} - \begin{bmatrix} b_1k_1 & b_1k_2 & b_1k_3 & b_1k_4 \\ b_2k_1 & b_2k_2 & b_2k_3 & b_2k_4 \\ b_3k_1 & b_3k_2 & b_3k_3 & b_3k_4 \\ b_4k_1 & b_4k_2 & b_4k_3 & b_4k_4 \end{bmatrix}$$

$$= \begin{bmatrix} a_{11}-b_1k_1 & a_{12}-b_1k_2 & a_{13}-b_1k_3 & a_{14}-b_1k_4 \\ a_{21}-b_2k_1 & a_{22}-b_2k_2 & a_{23}-b_2k_3 & a_{24}-b_2k_4 \\ a_{31}-b_3k_1 & a_{32}-b_3k_2 & a_{33}-b_3k_3 & a_{34}-b_3k_4 \\ a_{41}-b_4k_1 & a_{42}-b_4k_2 & a_{43}-b_4k_3 & a_{44}-b_4k_4 \end{bmatrix} = \begin{bmatrix} A_{11} & A_{12} & A_{13} & A_{14} \\ A_{21} & A_{22} & A_{23} & A_{24} \\ A_{31} & A_{32} & A_{33} & A_{34} \\ A_{41} & A_{42} & A_{43} & A_{44} \end{bmatrix}$$

$$\bar{A} = T\left(A - bk^T\right)T^{-1} = \begin{bmatrix} 1 & 0 & 0 & 0 \\ 0 & 1 & 0 & 0 \\ 0 & 0 & 1 & 0 \\ c_1 & c_2 & c_3 & c_4 \end{bmatrix} \begin{bmatrix} A_{11} & A_{12} & A_{13} & A_{14} \\ A_{21} & A_{22} & A_{23} & A_{24} \\ A_{31} & A_{32} & A_{33} & A_{34} \\ A_{41} & A_{42} & A_{43} & A_{44} \end{bmatrix} \begin{bmatrix} 1 & 0 & 0 & 0 \\ 0 & 1 & 0 & 0 \\ 0 & 0 & 1 & 0 \\ -\frac{c_1}{c_4} & -\frac{c_2}{c_4} & -\frac{c_3}{c_4} & \frac{1}{c_4} \end{bmatrix}$$

$$= \left[\begin{array}{ccc|c} A_{11} - A_{14}\frac{c_1}{c_4} & A_{12} - A_{14}\frac{c_2}{c_4} & A_{13} - A_{14}\frac{c_3}{c_4} & \frac{A_{14}}{c_4} \\ A_{21} - A_{24}\frac{c_1}{c_4} & A_{22} - A_{24}\frac{c_2}{c_4} & A_{23} - A_{24}\frac{c_3}{c_4} & \frac{A_{24}}{c_4} \\ A_{31} - A_{34}\frac{c_1}{c_4} & A_{32} - A_{34}\frac{c_2}{c_4} & A_{33} - A_{34}\frac{c_3}{c_4} & \frac{A_{34}}{c_4} \\ \hline M_1 - M_4\frac{c_1}{c_4} & M_2 - M_4\frac{c_2}{c_4} & M_3 - M_4\frac{c_3}{c_4} & \frac{M_4}{c_4} \end{array}\right]$$

where

$M_1 = c_1A_{11} + c_2A_{21} + c_3A_{31} + c_4A_{41}$

$M_2 = c_1A_{12} + c_2A_{22} + c_3A_{32} + c_4A_{42}$

$M_3 = c_1A_{13} + c_2A_{23} + c_3A_{33} + c_4A_{43}$

$M_4 = c_1A_{14} + c_2A_{24} + c_3A_{34} + c_4A_{44}$.